1-1-1972

Moire Patterns and Two-Dimensional Aliasing in Line Scanner Data Acquisition Systems

C. D. McGillem

T. E. Riemer

LARS Information Note 111772

Moiré Patterns and Two-Dimensional Aliasing in Line Scanner Data Acquisition Systems

by
C. D. McGillem
T. E. Riemer

The Laboratory for Applications of Remote Sensing

Purdue University
West Lafayette, Indiana

1973

MOIRÉ PATTERNS AND TWO-DIMENSIONAL ALIASING IN LINE SCANNER DATA ACQUISITION SYSTEMS

C. D. McGillem
T. E. Riemer

Abstract

The basic mechanism underlying the generation of Moiré patterns in line scanner data acquisition systems is examined. A general expression is developed in terms of typical system parameters for the reproduced image of such systems and the interaction of the image spectrum; the raster frequency and digital sampling frequency of the A/D conversion process are discussed and examples given. System design requirements for avoiding Moiré pattern generation and two-dimensional aliasing are discussed.

MOIRÉ PATTERNS AND TWO-DIMENSIONAL ALIASING IN LINE SCANNER DATA ACQUISITION SYSTEMS

I. Introduction:

The flying spot scanner and optical line scanner are widely used for converting visual or other two-dimensional radiant signals to electrical form for further processing. When this processing is accomplished by means of a digital computer, A/D conversion of the scanner analog output signal is required. Thus in effect, the original two-dimensional spatial signal is sampled along two approximately orthogonal axes: by the scanner raster in a direction normal to the scan lines, and by the A/D sampling in a direction parallel to the scan lines. Figure 1 shows a typical system of this type used for remote sensing of the earth's surface from an aircraft. The transverse motion of the field of view of the sensor is produced by a rotating mirror, while the forward motion is produced by the translation of the platform carrying the sensor. A/D conversion may be accomplished at the time of measurement or later at a data processing center from an analog recording of the scanner signal.

The measured signal can be reconstructed as a sampled raster by

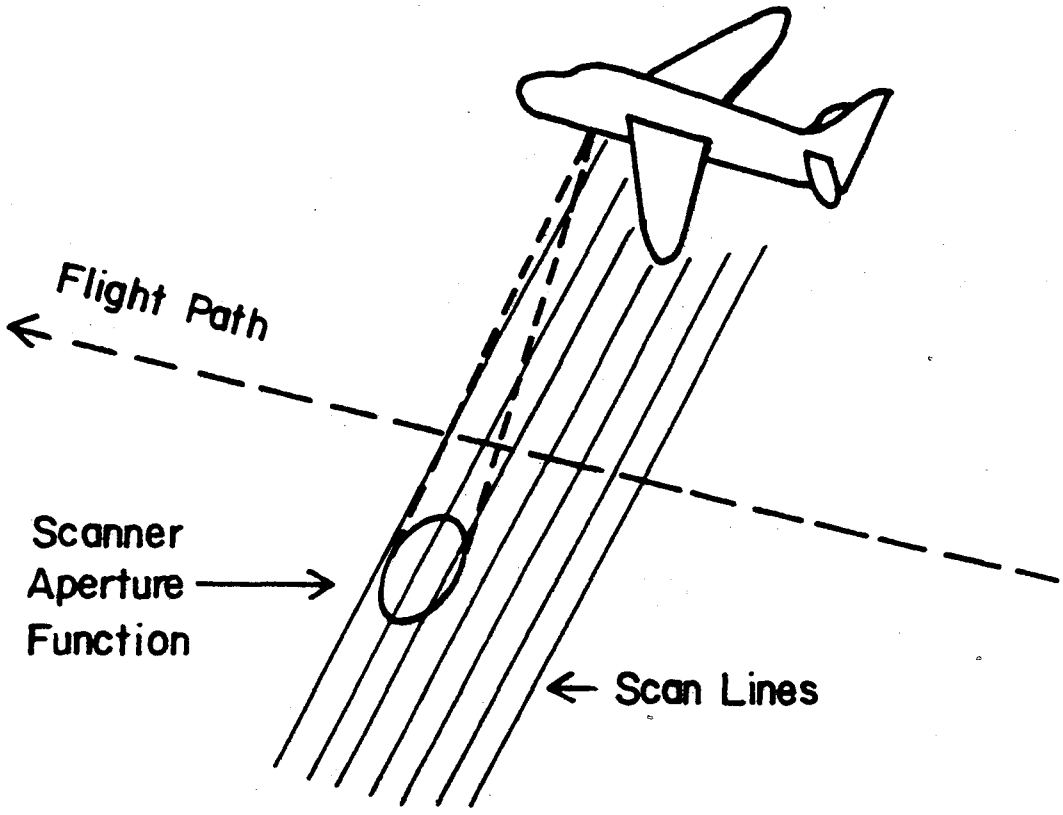

Figure 1. Basic Line Scanner Configuration Used in Remote Sensing of Earth's Surface.

intensity modulating a scanning light beam and recording the signal on photographic film or viewing it on a digital display. Figure 2 shows a typical picture recorded and reproduced in this manner. The signal was recorded by a line scanner operating in the infrared portion of the spectrum (0.62 to 0.66 μm). The scanner used to make the picture was carried in an aircraft flying at an altitude of 215 meters over typical farmland in central Indiana. It is evident in this picture that there has been distortion introduced in the form of Moiré patterns through much of the left center of the picture. Since the analog signal is low pass filtered to half the sampling rate of the A/D conversion process, the resulting Moiré patterns arise principally from the fact that sampling and reconstruction were carried out on a signal having significant spatial frequency components in excess of half the scan line or raster spatial sampling frequency. Thus, these Moiré patterns, because of the low pass filtering prior to the A/D conversion process, are primarily a form of one-dimensional aliasing. Figure 3 shows the magnitude of the two-dimensional Fourier transform of Fig. 2. Aliasing along the y-spatial frequency axis, corresponding to aliasing about integer multiples of the raster sampling frequency, is clearly evident. If the low pass filtering is inadequate, then the resulting Moiré patterns arise from two-dimensional aliasing.

This type of distortion is particularly insidious because it cannot be removed a posteriori without serious loss of information content of the picture. Its presence indicates that serious undersampling of the image has occurred and that it is impossible to accurately reproduce the picture by interpolating between sample points to obtain a continuous image. Limitations of this kind are particularly important in connection

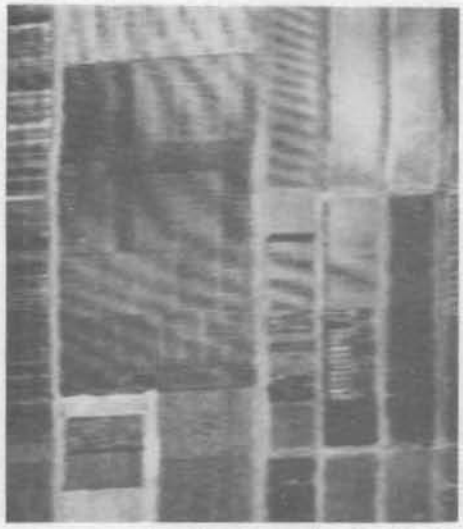

Figure 2. Line Scanner Picture of Earth's Surface (Run 66005202, Channel 1, Columns 11-256, Lines 511-766).

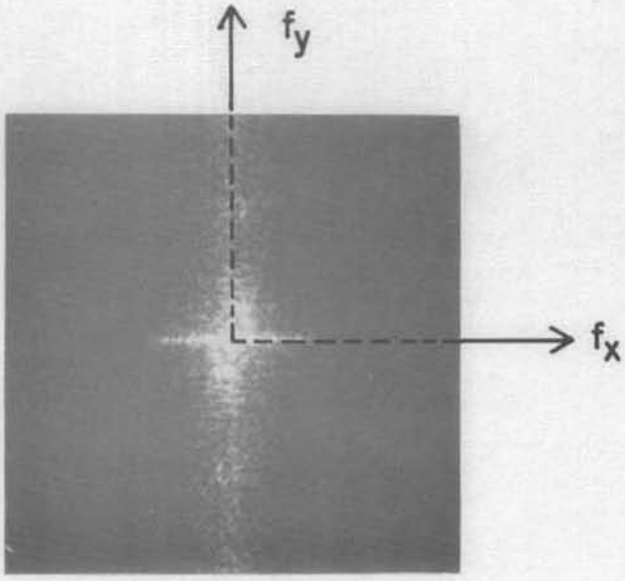

Figure 3. Modulus of the Two-Dimensional Fourier Transform of Figure 2.

with the problems of correcting geometrical distortion, registration of data from images recorded at different times, and combining geometrical and spectral characteristics of images to improve classification accuracy. The mathematical model of the process whereby this type of distortion is produced and certain of the methods for handling it are discussed in the following sections.

II. One-Dimensional Aliasing

The one dimensional aliasing problem will be considered first as an introduction to a more precise two-dimensional aliasing problem formulation. The generation of Moiré patterns by the analyzing of patterns containing periodic intensity variations has been known for centuries [12] and much analysis has been performed on this subject [4, 8, 10, 11]. This process can be modelled mathematically as the multiplication of two or more two-dimensional intensity functions containing spatial frequency components that are nearly equal to one another. In the case of a line scanner (or a TV system) where no A/D processing is involved, the resulting image is taken as the product of the intensity function of the image and the scanner intensity function. For this case a Moiré pattern will result whenever there are discrete spatial frequency components in the image that approach the spatial frequency components of the scanner function.

The basic mechanism whereby Moiré patterns are generated is most easily seen by considering the two-dimensional frequency spectra of the image and scanner functions. Let $\theta(x,y)$ be the intensity variation of the image as a function of the spatial coordinates x and y, $\varphi(x,y)$ be the intensity variation of the scanner function, and $\gamma(x,y)$ be the resulting intensity function of the scanned image. These functions can

be related by

$$\gamma(x,y) = \theta(x,y)\ \varphi(x,y) \tag{1}$$

Taking the two-dimensional Fourier transform of Eq. 1 gives the frequency spectrum of the scanned image as a two-dimensional convolution of the transforms of $\theta(x,y)$ and $\varphi(x,y)$; i.e.,

$$\Gamma(f_x,f_y) = \Theta(f_x,f_y) \ast\ast \Phi(f_x,f_y)\ , \tag{2}$$

where f_x and f_y are the spatial frequency variables of the Fourier transform. In order to more clearly illustrate the mechanism by which the new frequencies (Moiré patterns) are generated, it is convenient to consider the image function to be infinite in extent and the scanned image function to be the product of a raster function, $\varphi'(x,y)$, that is infinite in extent and a window function, $w(x,y)$, that is unity over the viewing area of the scanner and zero elsewhere. With these stipulations Eq. 1 can be rewritten as,

$$\begin{aligned}\gamma(x,y) &= \theta(x,y)\ \varphi'(x,y)\ w(x,y)\\ &= \mathcal{F}^{-1}\left\{\Theta(f_x,f_y) \ast\ast \Phi'(f_x,f_y)\right\} w(x,y).\end{aligned} \tag{3}$$

Thus the scanned image is just the inverse transform of the convolution of the image with the infinite extent raster function multiplied by the window function to limit the extent of the final image.

In order to illustrate in a simple manner the mathematical basis of the mechanism whereby Moiré patterns are generated, assume for the moment that the image intensity function and the line scanner function both vary in amplitude in a sinusoidal manner. The frequencies and spatial orientations for these two functions need not be the same. The two-dimensional Fourier transform of this type of function consists of

a pair of impulses corresponding to each sinusoidal component. Two representative functions and their transforms are shown in Fig. 4.

The product of the raster function and the image function has a transform given by the double convolution of the individual transforms. This is readily seen by inspection (since only impulses are involved) to consist of four impulses as shown in Fig. 5. The two impulses near the origin represent a low-frequency sinusoidal component. This component arises from one-dimensional aliasing of the y-spatial frequency components of the image intensity function about the y-frequency components of the raster function, and correspond to what is normally considered a Moiré pattern. This Moiré pattern has a frequency of

$$f_m = (f_i^2 + f_r^2 - 2 f_i f_r \cos \alpha)^{\frac{1}{2}} \tag{4}$$

and an angle with respect to the y-axis of

$$\beta = \sin^{-1} \frac{f_i \sin \alpha}{f_m} , \tag{5}$$

and would appear as shown in Fig. 5. If the high frequency component, f_h in Fig. 5, is not filtered out in the reconstruction process, it will also be visible as a sinusoidal intensity variation in a direction parallel to a line connecting the two impulses at f_h shown in Fig. 5. Further study of Fig. 5 makes it clear that there is considerable interdependence between the Moiré pattern and both the frequency and orientation of the generating signals. For example a change in orientation of one of the generating patterns can lead to a change in both the frequency and orientation of the Moiré pattern.

With this brief introduction a more precise formulation of the two-dimensional aliasing problem will now be made.

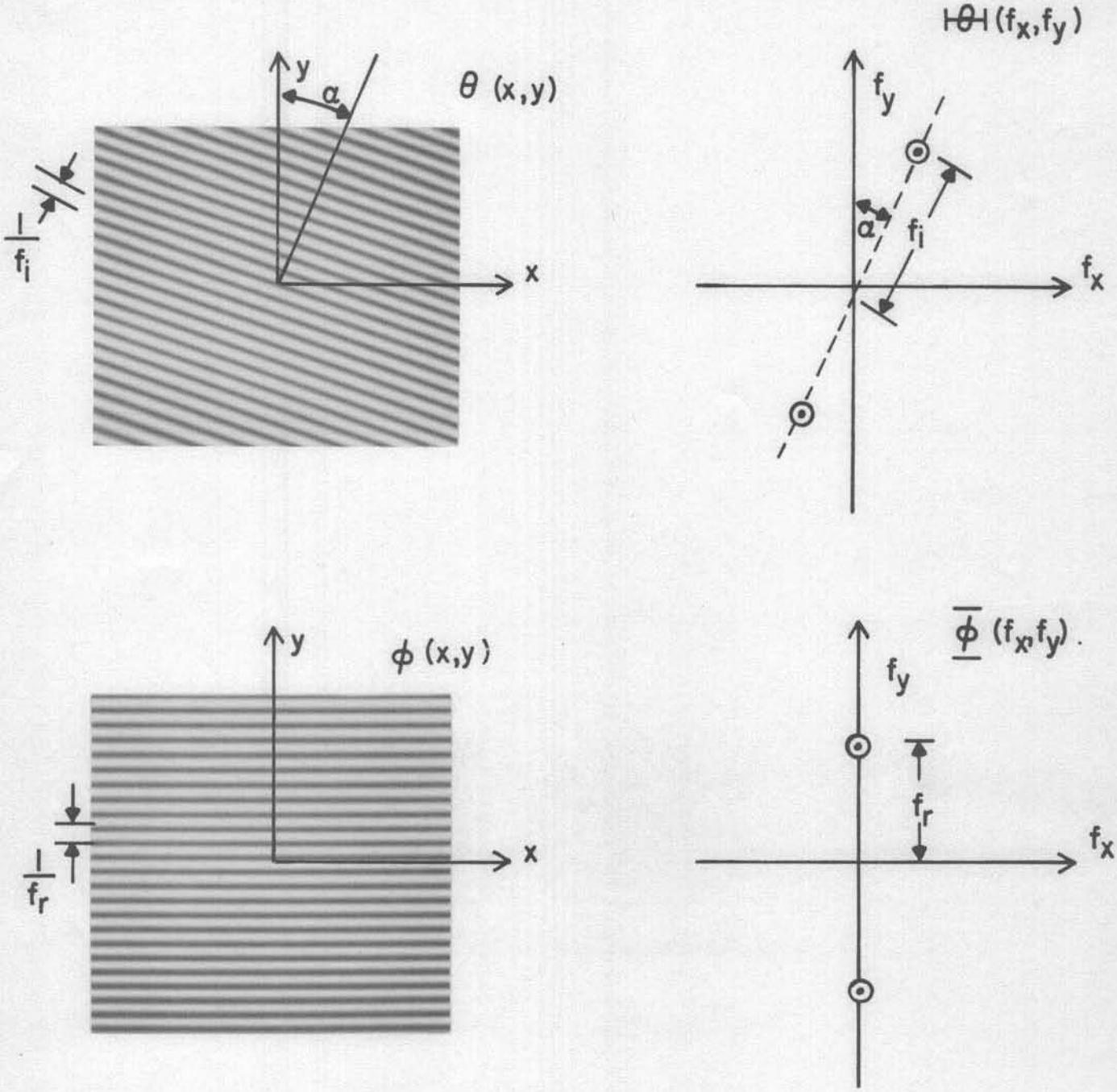

Figure 4. Sinusoidal Image and Raster Functions and Corresponding Two-Dimensional Fourier Transforms for $\alpha=1^{o}$ and $f_i=0.9792\ f_r$.

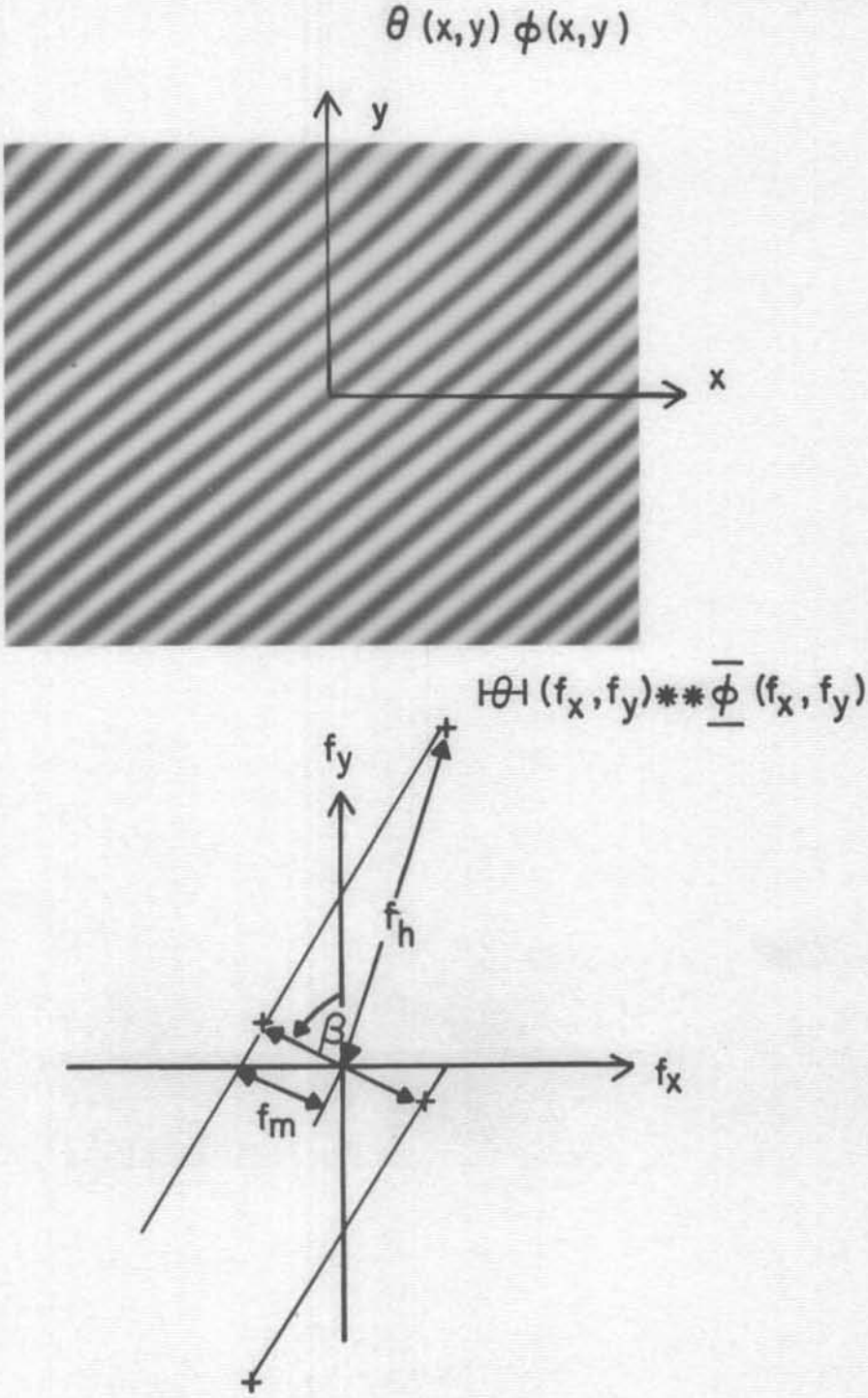

Figure 5. Moiré Pattern and Corresponding Two-Dimensional Fourier Transform Resulting from the Product of the Image and Raster Functions of Figure 4.

III. Scanner-Reproducer System

The block diagram of a typical line scanner and associated reproducing system is shown in Fig. 6. The variables in the system of Fig. 6 are defined as follows:

x_1, y_1 - coordinates of scanned image

$\theta_s(x_1, y_1)$ - intensity function of scanned image

$g_s(x_1, y_1)$ - aperture function of scanner

$u_1(t)$ - analog time varying output signal of scanner

$h(t)$ - impulse response of signal conditioning and/or low pass filter of A/D converter

$u_2(t)$ - analog output signal of signal conditioner

T_1 - period of sampling interval in A/D converter

x, y - coordinates of reproduced image

$g_r(x,y)$ - aperture function of reproducer

$\theta_r(x,y)$ - intensity function of reproduced image

The output signal from the scanner at any instant of time is the integral of the product of the aperture function and the image intensity function and is given by

$$u_1(t) = \sum_{n=-\frac{N}{2}}^{\frac{N}{2}} \int_{-\infty}^{\infty} \int_{-\infty}^{\infty} \theta_s(x_1, y_1)\, g_s\left[x_1 - v(t - nT),\ y_1 - n\Delta y\right] dx_1\, dy_1 \qquad (6)$$

where

$N + 1$ = number of scan lines in scanned image

v = velocity of scanner aperture in x_1 direction

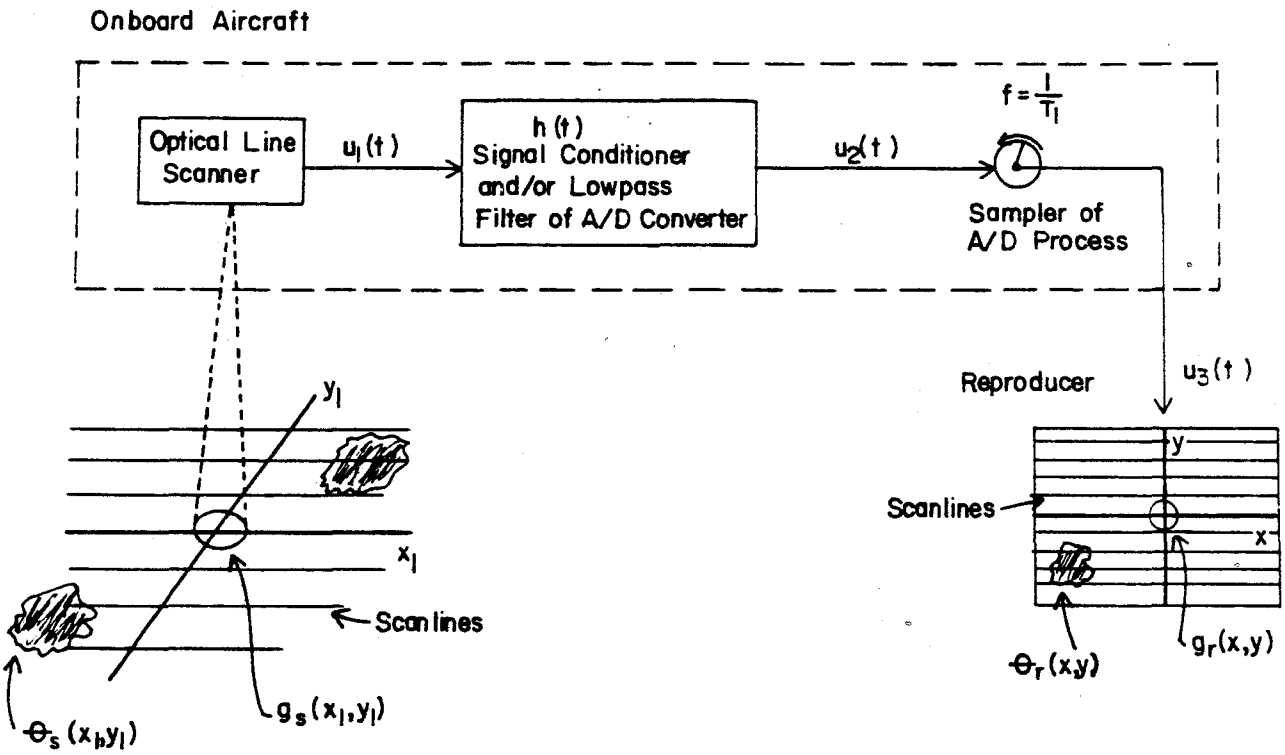

Figure 6. Scanner-Reproducer System.

Δy = distance between centers of consecutive scan lines measured in y_1 direction

T = time duration of one scan line.

The output of the signal conditioner, $u_2(t)$, is the convolution of $u_1(t)$ with $h(t)$ and can be expressed as

$$u_2(t) = u_1(t) * h(t)$$

$$= \int \sum_{n=-\frac{N}{2}}^{\frac{N}{2}} \iint \theta_s(x_1,y_1)\ g_s\left[(x_1 - v(t-\tau-nT),\ y_1 - n\Delta y\right]$$

$$h(\tau)\ dx_1\, dy_1\, d\tau\ . \qquad (7)\ \underline{/1}$$

The output of the sampler of the A/D conversion process, $u_3(t)$, can be approximated by

$$u_3(t) = u_2(t) \sum_{\alpha=-\frac{A}{2}}^{\frac{A}{2}} \delta(t - \alpha T_1) \qquad (8)$$

where

$A+1$ = number of samples of $u_2(t)$ taken during one scan line.

The reproduced image is given by a running average of the reproducer aperture function and the reproducer input signal, $u_3(t)$, as

$$\theta_r(x,y) = \sum_{m=-\frac{M}{2}}^{\frac{M}{2}} \int u_3(t)\ g_r\left[x - v(t-mT),\ y - m\Delta y\right] dt \qquad (9)$$

where $m+1$ = number of scan lines in reproduced image. Substituting Eq. 7 and 8 into 9, interchanging the order of integration and summation and noting that for synchronous reproduction of the raster

---

/1 All integrals are to be interpreted as having infinite limits unless otherwise specified.

the indices m and n are identical gives

$$\theta_r(x,y) = \sum_{n=-\frac{N}{2}}^{\frac{N}{2}} \sum_{\alpha=-\frac{A}{2}}^{\frac{A}{2}} \iiint \theta_s(x_1,y_1)\, g_s\left[x_1 - v(\alpha T_1 - \tau - nT),\, y_1 - n\Delta y\right]$$

$$g_r\left[x - v(\alpha T_1 - nT),\; y - n\Delta y\right] h(\tau)\, dx_1\, dy_1\, d\tau \;. \tag{10}$$

Considerable insight into the significance of the various factors in Eq. 10 can be gained by transforming to the spatial frequency domain. Taking the two-dimensional Fourier transform of Eq. 10 gives

$$\Theta_r(f_x,f_y) = G_r(f_x,f_y) \sum_{n=-\frac{N}{2}}^{\frac{N}{2}} \sum_{\alpha=-\frac{A}{2}}^{\frac{A}{2}} e^{-j\,2\pi[f_x v(\alpha T_1 - nT) + f_y\, n\Delta y]}$$

$$\iiint \theta_s(x_1,y_1)\, g_s\left[x_1 - v(\alpha T_1 - \tau - nT),\; y_1 - n\Delta y\right]$$

$$h(\tau)\, dx_1\, dy_1\, d\tau \;. \tag{11}$$

The triple integral of Eq. 11 can be recognized as a triple convolution. Rewriting Eq. 11 using convolutional notation

$$\Theta_r(f_x,f_y) = G_r(f_x,f_y) \sum_{n=-\frac{N}{2}}^{\frac{N}{2}} \sum_{\alpha=-\frac{A}{2}}^{\frac{A}{2}} e^{-j\,2\pi[f_x v(\alpha T_1 - nT) + f_y\, n\Delta y]}$$

$$\Big[\Big\{\theta_s[v(\alpha T_1 - nT), n\Delta y] \;**\; g_s[-v(\alpha T_1 - nT), -n\Delta y]\Big\}$$

$$* \; h(\alpha T_1 - nT)\Big] \tag{12}$$

where "**" denotes a two-dimensional convolution. Equation 12 can be

further simplified by writing the double summation as a double integral over a sum of impulses as follows

$$\Theta_r(f_x,f_y) = G_r(f_x,f_y) \iint \left[\left\{\theta_s[vx,y] \;\; g_s[-vx,-y]\right\} * h(x)\right] \cdot$$

$$\sum_{n=-\frac{N}{2}}^{\frac{N}{2}} \sum_{\alpha=-\frac{A}{2}}^{\frac{A}{2}} \delta(x-\alpha T_1+nT,\; y-n\Delta y)\; e^{-j\,2\pi(vf_x x+f_y y)}\, dx\, dy \tag{13}$$

and using the fundamental properties of convolution and multiplication of the Fourier transform to give

$$\Theta_r(f_x,f_y) = G_r(f_x,f_y)\left[H(f_x v)\,\Theta_s(f_x,f_y)\; G_s(-f_x,-f_y) \;\; Q(f_x,f_y)\right] \tag{14a}$$

where

$$Q(f_x,f_y) = \iint \sum_{n=-\frac{N}{2}}^{\frac{N}{2}} \sum_{\alpha=-\frac{A}{2}}^{\frac{A}{2}} \delta(x-\alpha T_1+nT,\; y-n\Delta y)\; e^{-j\,2\pi(vf_x x+f_y y)} dxdy$$

$$= \frac{\sin\pi(N+1)\,Tvf_x}{\sin\pi T\,vf_x}\;\frac{\sin\pi(A+1)\,T_1 vf_x}{\sin\pi T_1\,vf_x}\;\frac{\sin\pi(N+1)\,\Delta y\, f_y}{\sin\pi\Delta y\, f_y} \tag{14b}$$

In order to gain further insight into Eq. (14a), consider the limiting case in which $N\to\infty$ and $A\to\infty$. For this case Eq. (14b) becomes

$$\lim_{\substack{N\to\infty\\ A\to\infty}} Q(f_x,f_y) = \frac{1}{T_1 v}\sum_{\alpha=-\infty}^{\infty} \delta\left(f_x-\frac{\alpha}{T_1 v}\right)\frac{1}{\Delta y}\sum_{n=-\infty}^{\infty}\delta\left(f_y-\frac{n}{\Delta y}\right). \tag{15}$$

Using Eq. 15, Eq. 14a can be written as

$$\Theta_r(f_x,f_y) = \frac{G_r(f_x,f_y)}{vT_1\ \Delta y} \sum_{\alpha=-\infty}^{\infty} \sum_{n=-\infty}^{\infty} H\left[v\left(f_x - \frac{\alpha}{T_1 v}\right)\right] \Theta_s\left(f_x - \frac{\alpha}{T_1 v}, f_y - \frac{n}{\Delta y}\right)$$

$$G_s\left[-\left(f_x - \frac{\alpha}{T_1 v}\right), -\left(f_y - \frac{n}{\Delta y}\right)\right] . \qquad (16)$$

From Eq. 16 it is evident from the double summations that the reproduced image contains a superposition of frequency translates, at intervals of $\frac{1}{T_1 v}$ and $\frac{1}{\Delta y}$ along the f_x and f_y spatial frequency axes, respectively, of the product of the transfer functions of the analog signal conditioner and/or low pass filter of the A/D processor, the scanned image, and the scanner aperture. Each of these translates is weighted by the reproduction aperture transfer function. Figure 7 shows how the magnitude of $\Theta_r(f_x,f_y)$ in Eq. 16 might look. The degree to which portions of the replicated spectra overlap into the spectral band $-\frac{1}{2\Delta y} \le f_y \le \frac{1}{2\Delta y}$, $-\frac{1}{2T_1 v} \le f_x \le \frac{1}{2T_1 v}$ is the degree to which aliasing occurs and the degree to which image distortion occurs. If there are discrete components in the spectrum $H(vf_x)\ \Theta_s(f_x,f_y)$ $G_s(-f_x,-f_y)$ near any harmonics, $\frac{n}{\Delta y}$, of the raster frequency or, $\frac{\alpha}{T_1 v}$, of the A/D sampling process then these will appear in the reproduced image as low frequency components and correspond to what are usually called Moiré patterns. The absence of Moiré patterns in a reproduced image does not necessarily imply that no distortion is present, but only that it is not present as a spurious narrow-band isolated component.

Since it is impossible to remove aliasing from a sampled image, it is important to consider how to avoid the occurrence of this undesirable phenomenon. Such avoidance requires that the spectrum

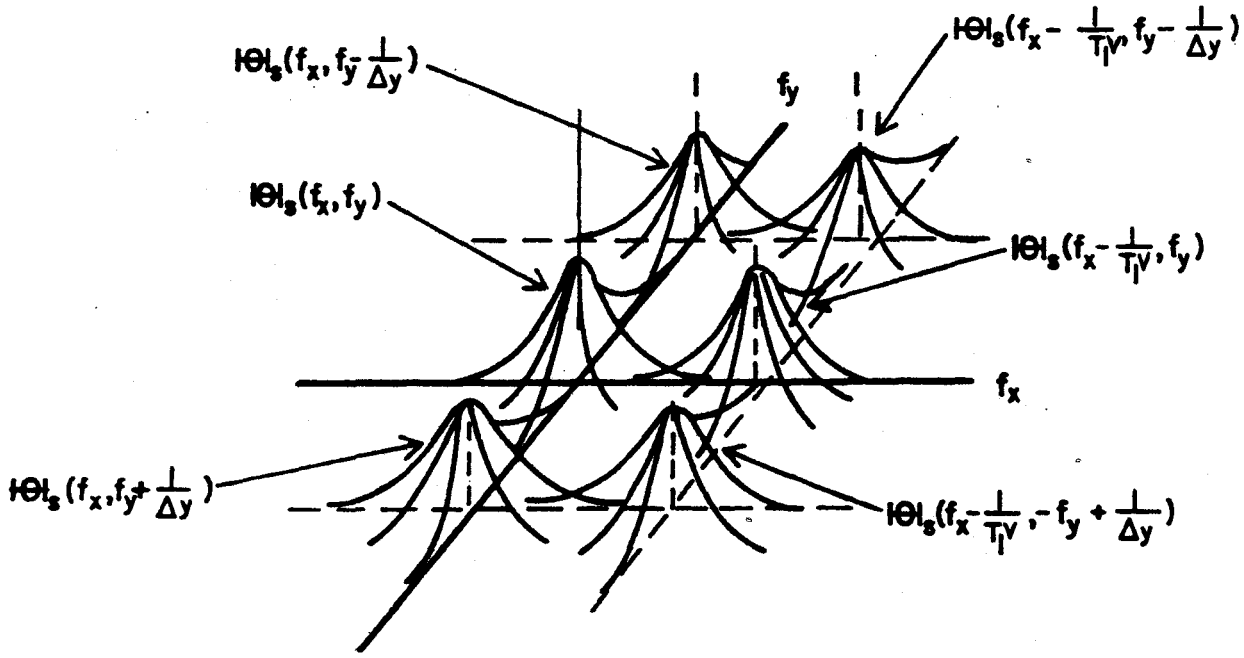

Figure 7. Partial Two-Dimensional Replication of the Original Image Spectral Components which Contribute to the Spectrum of the Reproduced Image.

$H(vf_x)\,\Theta_s(f_x,f_y)\,G_s(-f_x,-f_y)$ have no f_x components above $\frac{1}{2T_1v}$, and f_y components above $\frac{1}{2\Delta y}$. The factor $\Theta_s(f_x,f_y)$, the spectrum of the original image, is generally not under the control of the experimenter. Therefore, control of the spectrum must be accomplished by means of the temporal transfer function of the signal conditioner and/or low pass filter of the A/D process, $H(vf_x)$, and the scanner aperture transfer function, $G_s(f_x,f_y)$. By causing the product of $H(vf_x)\,G_s(-f_x,-f_y)$ to act as a low pass filter having a cutoff frequency of $\frac{1}{2T_1v}$ in the f_x direction and $\frac{1}{2\Delta y}$ in the f_y direction, all aliasing will be eliminated.

Achieving an approximation to the ideal low pass filter characteristic in the f_x direction is somewhat more easily accomplished because the spectral transmission in this direction is a function of the product $H(vf_x)\,G_s(-f_x,-f_y)$, while in the f_y direction all the filtering must be provided by $G_s(-f_x,-f_y)$. The primary constraints governing the choice of the impulse response of the analog signal conditioner (the A/D low pass filter), $h(t)$, are that it be causal and decay rapidly with time having no significant secondary lobes so as not to introduce any ghost images in the x-direction. However, an additional constraint is imposed upon the scanner aperture (or point spread function) for physical realizability, namely that it must not be negative. To simplify the discussion which follows, it will be assumed that $G_s(f_x,f_y)$ is symmetric with respect to the f_x and f_y axes. Thus the problem of choosing $G_s(f_x,f_y)$ so that the necessary low pass filtering in the f_y direction is obtained will be considered first.

Although not optimal, an excellent choice for $g_s(x,y)$ from the standpoint of realizability and shape of its frequency spectrum, $G_s(f_x,f_y)$, is a Hamming window function,

$$g_s(x,y) = 0.54 + 0.46 \cos \frac{2\pi}{z_o}(x^2+y^2)^{1/2} \quad , \text{ for } x^2+y^2 \leq \frac{z_o^2}{4} \tag{17}$$

$$= 0 \quad , \text{ otherwise}$$

where z_o is the diameter of the circular aperture. This function, $g_s(o,y)$, and its Fourier transform, $G_s(o,f_y)$ are shown in Fig. 8. The first null of $G_s(o,f_y)$ is at $f_y = \frac{2}{z_o}$ and this can be used to specify the width of the aperture z_o. Thus placing the first null of $G_s(o,f_y)$ at $\frac{1}{2\Delta y}$ specifies that $z_o = 4\Delta y$, or that the scanner aperture be four times the width of the spacing between the centers of adjacent scans of the image. Having specified $G_s(f_x,f_y)$, $H(vf_x)$ can be chosen so that the product $G_s(-f_x,-f_y)\,H(vf_x)$ approximates a low pass filter in the f_x direction with a cutoff frequency of $\frac{1}{2T_1v}$. Very often it is desirable to have equal spatial resolution along both axes, for such cases $T_1v = \Delta y$.

To illustrate the effectiveness of this filtering action in eliminating Moiré patterns, an image was generated, assuming $T_1v = \Delta y$, having two distinct sinusoidal frequency components. Figure 9a was generated by a low frequency sinusoid

$$f_L(x,y) = \cos 0.03\ \Delta y\ (x \sin 1^o + y \cos 1^o)$$

and Fig. 9b is the Moiré pattern produced by a high frequency sinusoid

$$f_H(x,y) = \cos 0.986\ \Delta y\ x\ .$$

Figure 9c is the sum of $f_L(x,y)$ and $f_H(x,y)$ after sampling and reconstruction using an impulse approximation for the scanner aperture $g_s(x,y)$. Figure 9d is the sum of $f_L(x,y)$ and $f_H(x,y)$ after sampling and reconstruction using the Hamming function of Eq. 17 for $g_s(x,y)$. It is clear that the low frequency Moiré distortion sinusoid (i.e., the vertical band of Fig. 9c) is almost completely removed in Fig. 9d.

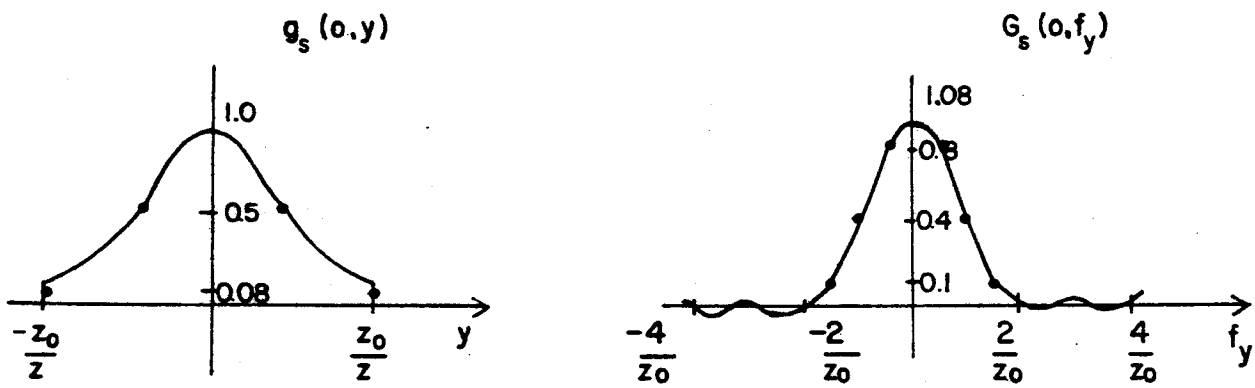

Figure 8. Hamming Window Function and Corresponding Fourier Transform.

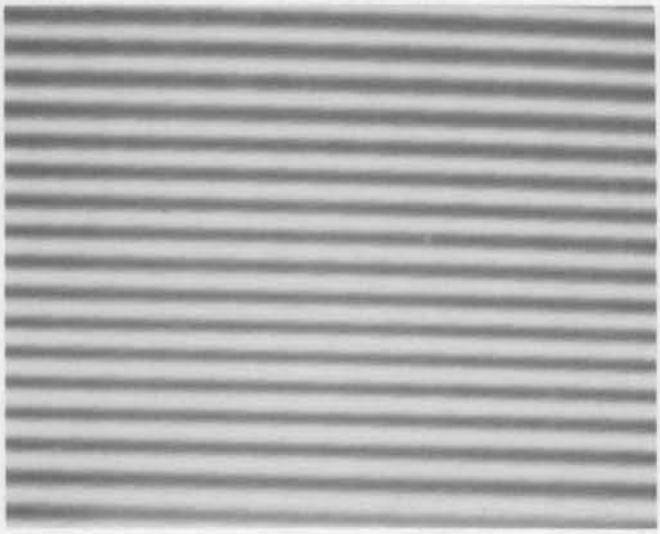

Figure 9a. Low Frequency Sinusoid.

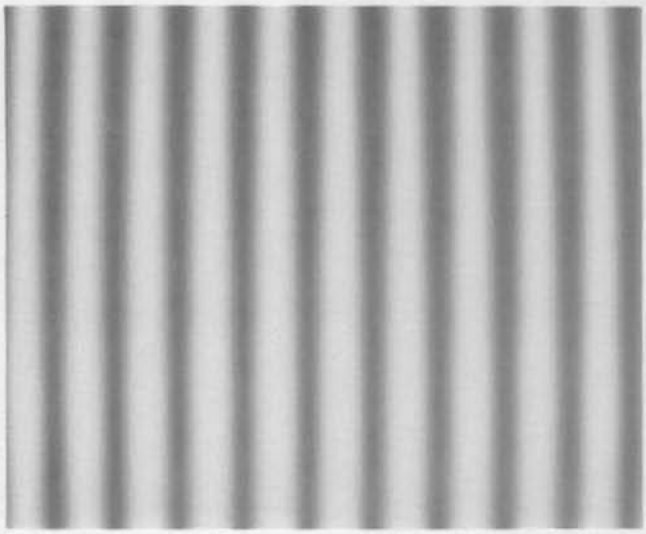

Figure 9b. Moiré Pattern Produced by a High Frequency Sinusoid and the Scanner Raster.

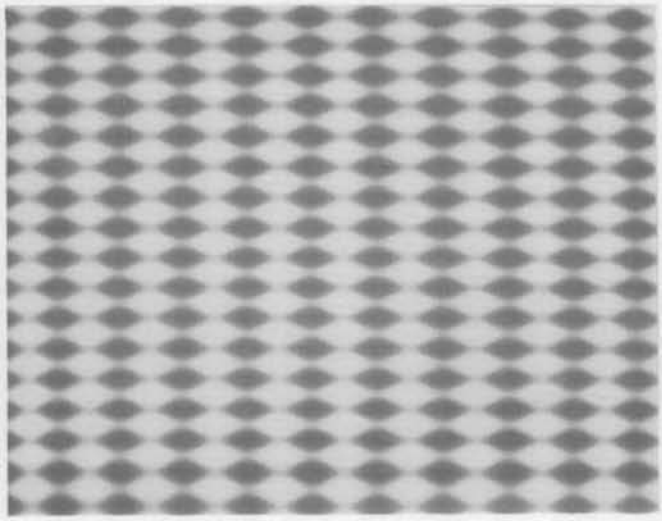

Figure 9c. Sum of the Low Frequency Sinusoid of Figure 9a and the Moiré Pattern of Figure 9b.

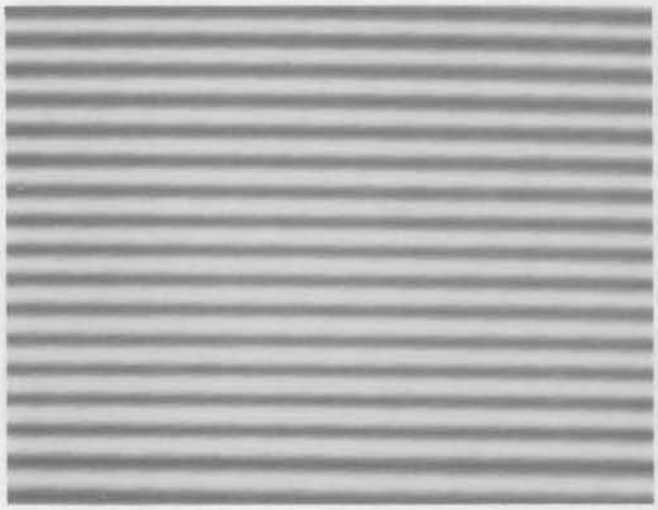

Figure 9d. Output of a Hamming Spatial Filter with the Components of Figure 9c as Input.

Figure 9. Example of Moiré Pattern Removal by a Hamming Spatial Filter.

IV. Conclusions

Moiré patterns appearing in the output of line scanner and digitally sampled data acquisition systems are a form of two-dimensional aliasing resulting from sampling at frequencies less than twice the highest spatial frequency components present in the original data. The existence of such patterns indicates that aliasing has occurred but their absence does not indicate an absence of aliasing, only that there are no discrete spatial frequency components in the data near a harmonic of the raster or sampling frequency. It is not possible to remove the distortion due to aliasing although specific components such as individual Moiré patterns can be removed by narrow band spatial frequency filters. The only adequate way to handle the distortion due to two-dimensional aliasing is to avoid it by proper design of the scanner aperture and by low pass filtering of the data before A/D conversion is carried out.

Bibliography

1. Ansley, D. A., "Resolution Testing of Coherent Optical Systems by Means of Linear Gratings," Applied Optics, Dec. 1970, pp. 2746-2752.

2. Bentler, F. J., "Alias-Free Randomly Timed Sampling of Stochastic Processes," I.E.E.E. Transactions on Information Theory, March 1970, pp. 147-152.

3. Blackman, R. B., and J. W. Tukey, The Measurement of Power Spectra, Dover, 1959.

4. Carter, W. H., "Aliasing in Sampled Holograms," Proceedings of the I.E.E.E., Jan. 1968, pp. 96-98.

5. Childers, D. G., "Study and Experimental Investigation in Sampling Rate and Aliasing in Time Division Telemetry Systems," I.R.E. Transactions on Space Electronics and Telemetry, Dec. 1962, pp. 267-283.

6. Landau, H. S., "Sampling, Data Transmission, and the Nyquist Rate," Proceedings of the I.E.E.E., Oct. 1967, pp. 1701-1706.

7. Macovski, A., "Spatial and Temporal Analysis of Scanned Systems," Applied Optics, August 1970, pp. 1906-1910.

8. Mertz, P. and F. Gray, "A Theory of Scanning and Its Relation to the Characteristics of the Transmitted Signal in Telephotography and Television," Bell System Technical Journal, July 1934, pp. 464-515.

9. Papoulis, A., Systems and Transforms with Applications in Optics, McGraw-Hill, 1968.

10. Rosen, L. "Moiré Effects in Computer-Generated Holograms," Proceedings of the I.E.E.E., Oct. 1967, pp. 1736-1737.

11. Sciammarella, C. A., "A Numerical Technique of Data Retrieval From Moiré or Photoelastic Patterns," Proceedings of the Society of Photo-Optical Instrumentation Engineers Pattern Recognition Studies Seminar, 1969, pp. 91-101.

12. Wolf, R. N., ed., Progress in Optics, vol. II, Wiley, 1964.